Microsc. Microanal. Page 1 of 5
doi:10.1017/S1431927613013652

Microscopy AND Microanalysis

Work Function Maps and Surface Topography Characterization of Nitroaromatic-Ended Dendron Films on Graphite

Eliana D. Farías,[1] Verónica Brunetti,[1,*] Julieta I. Paez,[2] Miriam C. Strumia[2], Mario C.G. Passeggi, Jr.,[3,4] and Julio Ferrón[3,4]

[1]*Departamento de Fisicoquímica (INFIQC-CONICET), Facultad de Ciencias Químicas, Universidad Nacional de Córdoba, Córdoba, X5000HUA, Argentina*
[2]*Departamento de Química Orgánica (IMBIV-CONICET), Facultad de Ciencias Químicas, Universidad Nacional de Córdoba, Córdoba, X5000HUA, Argentina*
[3]*Laboratorio de Superficies e Interfaces (IFIS Litoral, CONICET-UNL), Facultad de Ingeniería Química, Universidad Nacional del Litoral, Santa Fe, S3000GLN, Argentina*
[4]*Departamento de Materiales, Facultad de Ingeniería Química, Universidad Nacional del Litoral, Santa Fe, S3000AOM, Argentina*

Abstract: Surface topography and work function maps were simultaneously obtained for carbon surfaces modified by a dendritic molecule: 3,5-Bis (3,5-dinitrobenzoylamino) benzoic acid. The dendrons were spontaneously assembled onto highly ordered pyrolytic graphite samples, exhibiting an increase in the surface potential. This fact is consistent with the incorporation of an electron-acceptor functional group that remains electroactive on the surface.

Key words: dendron, self-assembly, Kelvin probe force microscopy, atomic force microscopy, work function

Introduction

The interaction of metals with organic layers has received considerable attention due to its importance in determining the reliability and durability of many technological devices and its relevance to future applications based on hybrid organic/inorganic nanoscale systems (Heimel et al., 2008; Hughes & Engstrom, 2010; Bélanger & Pinson, 2011; Kim et al., 2012). In this context, surface modification by adsorption of molecules from solutions is a simple route to obtain devices in a wide range of applications (Hasobe, 2012). Tailored nanostructured surfaces having good control over the morphology and other surface properties such as wettability, roughness, chemical reactivity, hardness, etc. can be obtained (Florio et al., 2012; Xu et al., 2012*b*). A common approach to amplify the effective area and quantity of functional groups is to graft dendritic molecules (Love et al., 2006; Peleshanko & Tsukruk, 2008; Park et al., 2011; Paez et al., 2012). On account of their controllable geometry, size, and functionality, dendrons are of considerable interest for surface modification and enlargement of active surfaces. However, targeted control of surface architecture requires an understanding of dendron/dendron and dendron/surface interactions, as well as in-depth knowledge of the structure of the dendrons in the solid state (Paez et al., 2012).

Supramolecular fabrications with two-dimensional networks are of great interest because such patterns provide the possibility to immobilize functional guest molecules. Carbon materials are widely used for a vast range of applications, from charge storage to catalyst supports (Cullen et al., 2012). Many of these applications rely on the ability to control the interfacial properties of carbon. For example, surface groups on carbon scaffolds can be used to anchor biomolecules or nanomaterials to achieve complex functionality. Thus, atomically flat highly oriented pyrolytic graphite (HOPG) surfaces are frequently chosen as substrates due to their advantageous properties, such as good conductivity and resistance to chemical or electrochemical attack (Yilmaz et al., 2009). During self-assembly, hydrogen bonding, dipolar or van der Waals interactions are always present as competing forces to dominate the supramolecular order (Klosterman et al., 2009; Xu et al., 2012*a*; Yang et al., 2012). A better understanding of noncovalent interactions will lead to the improved ability to predict and control the destiny of the surface-supported supramolecular layer (Palermo & Samorì, 2007; Surin et al., 2007). Hydrogen bonds, as one typical noncovalent bond, have been proven to be able to guide the self-assembly and to enhance the stability of the layers (De Feyter & De Schryver, 2003; Yoosaf et al., 2009; Ramesh & Thomas, 2010). For example, aromatic rings of 2,6-naphthalenedicarboxylic acid (NCD) and 4,4-biphenyldicarboxylic acid (BDC) molecules take the same orientation as that of a HOPG substrate to get maximum π–π attractive interactions between the adsorbed molecules and substrate, but while the NDC molecules form an incommensurate structure, the BDC molecules form a commensurate one (Pei et al., 2010). While the whole carboxyl group is invisible on the HOPG surface, the carboxylic carbon is visible on a gold one (Pei et al., 2010). In addition, the varying molecular orientation with the film thickness affects the evolution

Received April 19, 2013; accepted September 12, 2013
*Corresponding author. E-mail: verobrunetti@gmail.com

of the electronic properties (Ivančo, 2012). Two extreme orientations are of particular interest: molecules with their molecular planes parallel or near parallel to the substrate surface are referred to as lying oriented, while molecules with their molecular planes and/or backbones parallel or near parallel with the surface normal are oriented upright.

Kelvin probe force microscopy (KPFM) is a scanning probe microscopy method that provides us with the surface potential of a layer (Hoppe et al., 2005; Wei et al., 2010; Melitz et al., 2011; Matis et al., 2012). For example, it has been used to obtain the local work function of many electrodes from top-emitting organic light-emitting devices (Kim et al., 2011) and to show local voltage drops in graphene sheets (Yan et al., 2011). The surface potential of a molecular film is strongly related to its structure, terminal functional groups, orientation, packing density, etc. (Saito et al., 2001). Thus, depending on the way the molecules are polarized, a double layer may be expected with either a positive or negative surface potential toward the vacuum. The modulation of the surface density of states through self-assembly is a key phenomenon for obtaining new materials with tuned work functions. Interestingly, by appropriate choice of the molecules for functionalization, work function engineering can lead to work function values higher or lower than that for pristine materials. For instance, this could be of great interest for adjusting the work function of transparent electrodes to active layers in many optoelectronic devices (Reddy & Deepa, 2012; Spadafora et al., 2012).

The nitro-terminated dendron: 3,5-Bis (3,5-dinitrobenzoylamino) benzoic acid (D-NO_2) spontaneously adsorbs from μmol dimethylsulfoxide (DMSO) solutions onto carbon surfaces forming separated aggregates at the first stages and complete layers after only a few minutes (Paez et al., 2009). In this article, we use atomic force microscopy (AFM) to study its assembly morphology and KPFM to simultaneously obtain work function maps of the modified HOPG surface. The effect of an electron-acceptor functional group in the layer is evaluated through their electrical properties.

Materials and Methods

Materials

The synthesis of dendron D-NO_2 was performed following Kakimoto's procedure by using 3,5-diaminobenzoic acid and 3,5-dinitrobenzoyl chloride in DMAc (Ishida et al., 2000; Paez et al., 2008). All other commercially available chemicals were reagent grade and were used without further purification. All solutions were prepared immediately before their use. Water was purified with a Millipore Milli-Q system.

Scanning Probe Microscopy

AFM and KPFM images were acquired with a commercial Nanotec Electronic System operating in tapping mode at atmospheric pressure and room temperature. Acquisition and image processing were performed using the WS × M free software (Horcas et al., 2007). Budget Sensors Multi75E cantilevers with an electrically conductive coating of 5 nm chromium and 25 nm platinum on both sides of the tip, resonance frequency in the range of 60–90 kHz, nominal force constant in the range of 1–7 N/m, and radius smaller than 25 nm, were used. Samples for analysis were prepared by immersing fresh cleaved HOPG in a DMSO solution containing D-NO_2. They were subsequently rinsed with copious volumes of ethanol and water, dried under nitrogen flux and analyzed immediately. The experiment consisted of using AFM and KPFM imaging of samples submitted to different dipping times and concentrations.

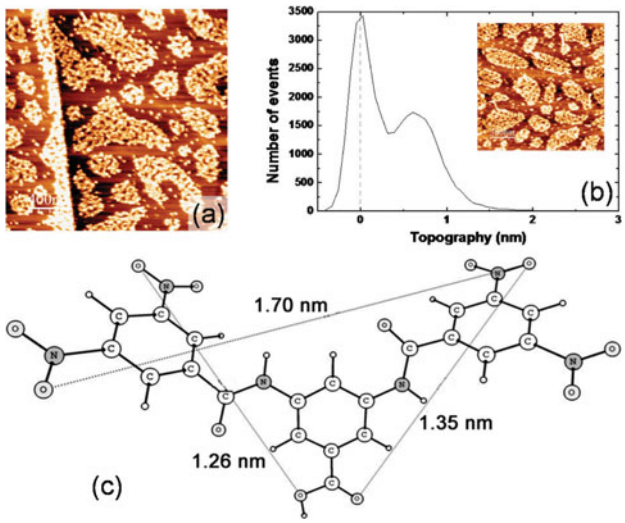

Figure 1. a: Atomic force microscopy (AFM) topographical image (2,000 × 2,000 nm) of a modified highly ordered pyrolytic graphite surface incubated in a 1 mmol/L D-NO_2 solution for 30 s. **b**: Surface roughness profile of the AFM image (1,800 × 1,800 nm) shown in the inset. **c:** Structure of D-NO_2 optimized in vacuum.

Results and Discussion

Dendron Layer Formation

AFM measurements were carried out to study the dendron layers adsorbed on HOPG substrates, in order to obtain topographical information, varying the incubation time and concentration of the dendron solution. It was observed that the surface is completely covered at concentrations higher than 1 mmol/L, even at very short times of incubation (time range in seconds) (Paez et al., 2009). Thus, samples were prepared at low incubation times in dilute solutions (0.1 and 1 mmol/L), which were conditions where low to intermediate coverage was obtained.

Figure 1a shows an AFM image of HOPG incubated 30 s in 1 mmol/L D-NO_2/DMSO. Nanometer features due to the adsorption of dendrons are observed. They appear as both isolated and aggregated features. In tapping mode, low tip–sample interactions allow the reproducible and repetitive imaging of the same surface area without any apparent distortion. It clearly shows the presence of islands formed by aggregates that nucleate exhibiting a strong interaction among them, and HOPG regions which remain uncovered. In addition, D-NO_2 molecules seem to decorate

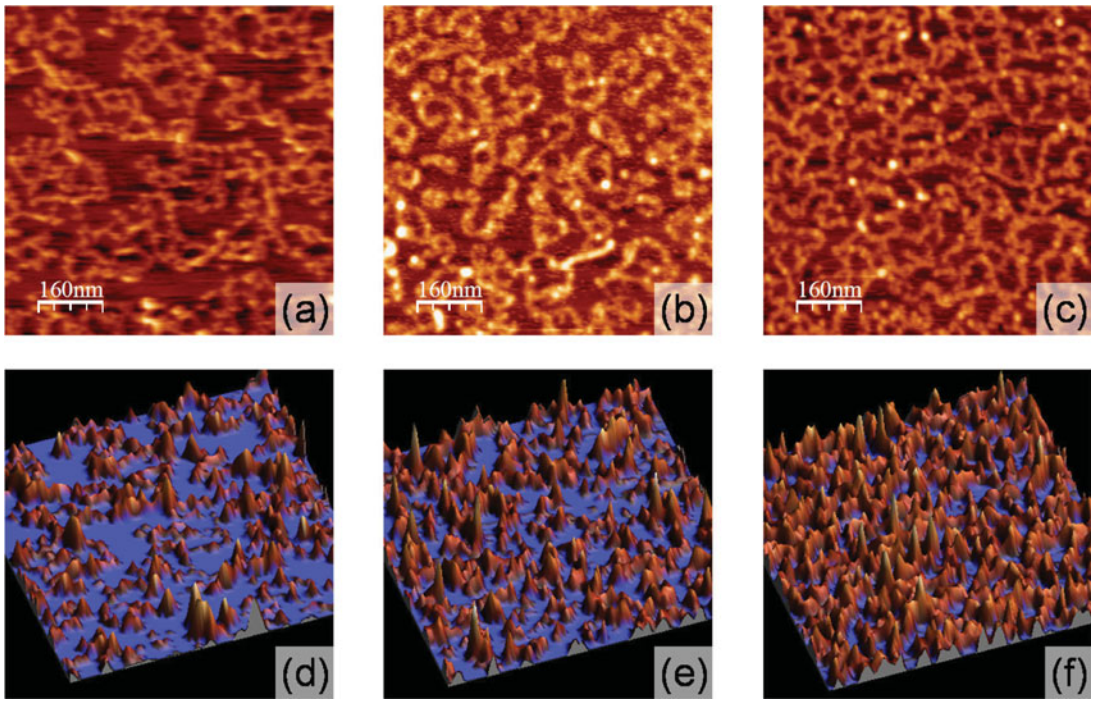

Figure 2. Atomic force microscopy topographical images (800 × 800 nm) of a modified highly ordered pyrolytic graphite surface incubated in a 0.3 mmol/L D-NO_2 solution at increasing times: (**a**) 15, (**b**) 60, and (**c**) 120 s and their corresponding 3D-flooding analysis images: (**d**) 15, (**e**) 60, and (**f**) 120 s.

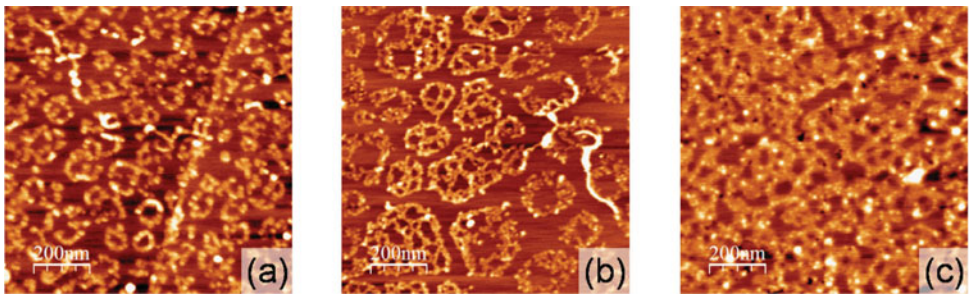

Figure 3. Atomic force microscopy topographical images (1,000 × 1,000 nm) of a modified highly ordered pyrolytic graphite surface incubated for 30 s at different D-NO_2/DMSO solution concentrations: (**a**) 0.3, (**b**) 1.0, and (**c**) 5.0 mmol/L.

mainly the upper side of the step-edge. The histogram of the heights of the dendron structure obtained from the inset image is plotted in Figure 1b and its calculated molecular size using Gaussian software is depicted in Figure 1c. Assuming that bare HOPG has an average height value of zero, D-NO_2 height values range between 0.5 and 1.5 nm, which suggests different adsorption geometries and likely different dendron–substrate interactions. In fact, the most probable height of D-NO_2 was found to be *ca*. 0.6 nm. This indicates that dendrons tend to aggregate in a tilted configuration favored by π–π stacking interactions between aromatic rings of neighbors themselves and with the HOPG substrate.

Figures 2a–2c shows the surface topography obtained after increasing the incubation time of HOPG in 0.3 mM D-NO_2 solution from 15 to 120 s. Although the formed structures seem to change their size and shape along the evolution, their height remains almost constant. The quantity of aggregates increased with increasing adsorption time, and larger domains of the dendron layer were formed. Figure 2d exhibits the 3D image of a flooding analysis performed to Figure 2a showing an occupied area of 42 ± 4% of hills after an incubation of 15 s. For 60 s, the occupied area grows up to 54 ± 2%; reaching a value of 67 ± 2% for 120 s (Figs. 2e, 2f). Similar trends are observed for HOPG surfaces incubated in solutions where dendron concentrations are increased at fixed incubation times (Fig. 3). In this case, an interesting organization is observed, where molecules which form circles in the most diluted stage (Fig. 3a) seem to join by strong adsorbate–adsorbate interactions that form a cross-linked network that maintains unchanged the shape of the formed structure after incubation in a 1 mM dendron solution (Fig. 3b). For more concentrated solutions, the network becomes distorted and tend to disappear, exhibiting a sort of noncoalesced dendron layer (Fig. 3c).

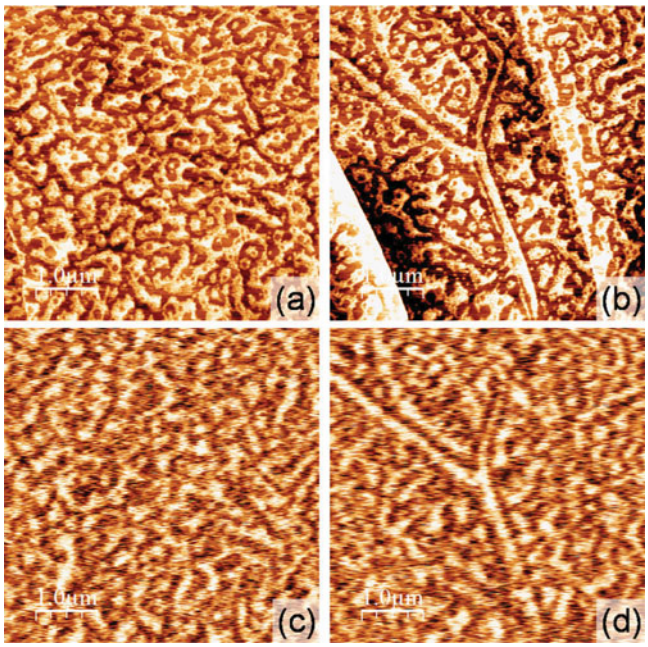

Figure 4. Atomic force microscopy images (5,000 × 5,000 nm) of a modified highly ordered pyrolytic graphite surface incubated in a 1 mmol/L D-NO_2/DMSO solution for 60 s, (**a–b**) topographical and (**c–d**) their corresponding Kelvin probe force microscopy images.

Kelvin Maps of Dendron Domains

The KPFM technique is a nondestructive procedure for investigation of molecular electrical properties that measure surface distribution of the potential. The technique is highly sensitive to the presence of surface dipoles, in particular for organic molecules (Hattori et al., 2010). Although KPFM has a superb sensitivity to measure variation of the potential along a surface, the absolute measurement of surface potential needs knowledge of the work function of the probe. Thus, calibration of the KPFM probe on a sample with a well-defined work function is required. Therefore, two measurements are needed, a first one over a reference surface and a second one over the sample under study (Melitz et al., 2011). In this article, the known work function surface of a bare HOPG surface (Melitz et al., 2011) is used as a reference. The corresponding KPFM images after the incubation of HOPG surfaces in D-NO_2 solutions allow us to report a general increase of the surface potential in the positions occupied by the nitroaromatic-ended dendrons.

Morphology and surface potential images are shown in Figure 4. As expected, it is known that the spatial resolution in the Kelvin map is lower than in the topography image due to the longer range of electrical forces relative to Van der Waals forces. In measuring electric and magnetic forces with an AFM, one needs to be sure of its origin, mainly when topographic and potential (magnetic) images have the same aspect, as in this work. The disappearance of step-edges in the KPMF images (see Figs. 4b, 4d) is clear evidence of its electrostatic origin, since different heights due to step-edges do not originate different potentials.

The dark and light domains in the KPFM images, Figures 4c and 4d, correspond to low and high surface potentials in each sample, respectively. Note that the Kelvin maps are not as heterogeneous, with values of the Kelvin voltage varying between −0.020 and 0.020 V. Thus, the surface potential for the dendron film was *ca*. 0.040 V more positive than that of the HOPG substrate for a sub-monolayer deposit, whereas the difference grows up to 0.110 V for complete coverage layers (not shown). At this point, it is important to note that the change in the surface potential is related not only to the chemical composition of the layer, but also to its structure. Using HOPG as the standard reference surface for work measurements in air, we use the literature value of $WF_o = 4.475$ eV as the reference value (Hansen & Hansen, 2001), in order to estimate the average dendron covered surface work function in 4.515 to 4.585 eV depending on the incubation time.

Conclusions

Surface topography and work function images were simultaneously obtained by using AFM and KPFM techniques. The AFM images obtained after the incubation of HOPG samples in D-NO_2/DMSO showed the formation of a network film with embedded aggregates that completely covered the HOPG surface. The average height suggests a tilted preferred adsorption for the molecules, as well as a preferential upper side-step decoration. Increasing either the incubation time or the dendron concentration, the quantity of both network and aggregates increased. The corresponding KPFM images show a general increase in the surface potential in the positions occupied by the nitroaromatic-ended dendrons, as expected for the incorporation of an electron-acceptor functional group onto the surface. We believe that these results may be helpful in the design of nanoscale electronic and optoelectronic devices by using nitro-ended dendrons.

Acknowledgments

We wish to express our gratitude to Diego Andrada for his valuable help with Gaussian calculations. Financial support from CONICET, ANPCyT, and SECYT-UNC is gratefully acknowledged. E.I.F. and J.I.P. thank CONICET for their fellowships.

References

Bélanger, D. & Pinson, J. (2011). Electrografting: A powerful method for surface modification. *Chem Soc Rev* **40**(7), 3995–4048.

Cullen, R.J., Jayasundara, D.R., Soldi, L., Cheng, J.J., Dufaure, G. & Colavita, P.E. (2012). Spontaneous grafting of nitrophenyl groups on amorphous carbon thin films: A structure-reactivity investigation. *Chem Mater* **24**(6), 1031–1040.

De Feyter, S. & De Schryver, F.C. (2003). Two-dimensional supramolecular self-assembly probed by scanning tunneling microscopy. *Chem Soc Rev* **32**(3), 139–150.

Florio, G.M., Stiso, K.A. & Campanelli, J.S. (2012). Surface patterning of benzenecarboxylic acids: Influence of structure, solvent, and concentration on molecular self-assembly. *J Phys Chem C* **116**(34), 18160–18174.

Hansen, W.N. & Hansen, G.J. (2001). Standard reference surfaces for work function measurements in air. *Surf Sci* **481**(1–3), 172–184.

Hasobe, T. (2012). Photo- and electro-functional self-assembled architectures of porphyrins. *Phys Chem Chem Phys* **14**(46), 15975–15987.

Hattori, S., Kano, S., Azuma, Y. & Majima, Y. (2010). Surface potential of 1,10-decanedithiol molecules inserted into octanethiol self-assembled monolayers on Au(111). *J Phys Chem C* **114**(18), 8120–8125.

Heimel, G., Romaner, L., Zojer, E. & Bredas, J.L. (2008). The interface energetics of self-assembled monolayers on metals. *Acc Chem Res* **41**(6), 721–729.

Hoppe, H., Glatzel, T., Niggemann, M., Hinsch, A., Lux-Steiner, M.C. & Sariciftci, N.S. (2005). Kelvin probe force microscopy study on conjugated polymer/fullerene bulk heterojunction organic solar cells. *Nano Lett* **5**(2), 269–274.

Horcas, I., Fernández, R., Gómez-Rodríguez, J.M., Colchero, J., Gómez-Herrero, J. & Baro, A.M. (2007). WSXM: A software for scanning probe microscopy and a tool for nanotechnology. *Rev Sci Instrum* **78**(1), 013705-1–013705-9.

Hughes, K.J. & Engstrom, J.R. (2010). Interfacial organic layers: Tailored surface chemistry for nucleation and growth. *J Vac Sci Technol A* **28**(5), 1033–1059.

Ishida, Y., Jikei, M. & Kakimoto, M.A. (2000). Rapid synthesis of aromatic polyamide dendrimers by an orthogonal and a double-stage convergent approach. *Macromolecules* **33**(9), 3202–3211.

Ivančo, J. (2012). Intrinsic work function of molecular films. *Thin Solid Films* **520**(11), 3975–3986.

Kim, S.I., Oh, H.W., Huh, J.W., Ju, B. & Lee, C.W. (2011). Surface potential behaviors of UV treated of Ag anode for high-performance T-OLED by nanotribology. *Thin Solid Films* **519**(20), 6872–6875.

Kim, T.W., Yang, Y., Li, F. & Kwan, W.L. (2012). Electrical memory devices based on inorganic/organic nanocomposites. *NPG Asia Mater* **4**(6), e18-1–e18-12.

Klosterman, J.K., Yamauchi, Y. & Fujita, M. (2009). Engineering discrete stacks of aromatic molecules. *Chem Soc Rev* **38**(6), 1714–1725.

Love, C.S., Ashworth, I., Brennan, C., Chechik, V. & Smith, D.K. (2006). Dendron-protected Au nanoparticles—effect of dendritic structure on chemical stability. *J Colloid Interface Sci* **302**(1), 178–186.

Matis, B.R., Burgess, J.S., Bulat, F.A., Friedman, A.L., Houston, B.H. & Baldwin, J.W. (2012). Surface doping and band gap tunability in hydrogenated graphene. *ACS Nano* **6**(1), 17–22.

Melitz, W., Shen, J., Kummel, A.C. & Lee, S. (2011). Kelvin probe force microscopy and its application. *Surf Sci Rep* **66**(1), 1–27.

Paez, J.I., Froimowicz, P., Baruzzi, A.M., Strumia, M.C. & Brunetti, V. (2008). Attachment of an aromatic dendritic macromolecule to gold surfaces. *Electrochem Commun* **10**(4), 541–545.

Paez, J.I., Martinelli, M., Brunetti, V. & Strumia, M.C. (2012). Dendronization: A useful synthetic strategy to prepare multifunctional materials. *Polymers* **4**(1), 355–395.

Paez, J.I., Strumia, M.C., Passeggi, M.C.G., Jr., Ferrón, J., Baruzzi, A.M. & Brunetti, V. (2009). Spontaneous adsorption of 3,5-bis(3,5-dinitrobenzoylamino) benzoic acid onto carbon. *Electrochimica Acta* **54**(17), 4192–4197.

Palermo, V. & Samorì, P. (2007). Molecular self-assembly across multiple length scales. *Angewandte Chemie—Int Ed* **46**(24), 4428–4432.

Park, C., Lee, J. & Kim, C. (2011). Functional supramolecular assemblies derived from dendritic building blocks. *Chem Commun* **47**(44), 12042–12056.

Pei, Z., Lin, L., Zhang, H., Zhang, L. & Xie, Z. (2010). Self-assembly of 2,6-naphthalenedicarboxylic acid and 4,4′-biphenyldicarboxylic acid on highly oriented pyrolytic graphite and Au(1 1 1) surfaces. *Electrochimica Acta* **55**(27), 8287–8292.

Peleshanko, S. & Tsukruk, V.V. (2008). The architectures and surface behavior of highly branched molecules. *Prog Polym Sci (Oxford)* **33**(5), 523–580.

Ramesh, A.R. & Thomas, K.G. (2010). Directional hydrogen bonding controlled 2D self-organization of phenyleneethynylenes: From linear assembly to rectangular network. *Chem Commun* **46**(20), 3457–3459.

Reddy, B.N. & Deepa, M. (2012). Unraveling nanoscale conduction and work function in a poly(3,4-ethylenedioxypyrrole)/carbon nanotube composite by Kelvin probe force microscopy and conducting atomic force microscopy. *Electrochimica Acta* **70**, 228–240.

Saito, N., Hayashi, K., Sugimura, H., Takai, O. & Nakagiri, N. (2001). Surface potentials of patterned organosilane self-assembled monolayers acquired by Kelvin probe force microscopy and ab initio molecular calculation. *Chem Phys Lett* **349**(3–4), 172–177.

Spadafora, E.J., Saint-Aubin, K., Celle, C., Demadrille, R., Grévin, B. & Simonato, J.P. (2012). Work function tuning for flexible transparent electrodes based on functionalized metallic single walled carbon nanotubes. *Carbon* **50**(10), 3459–3464.

Surin, M., Samorì, P., Jouaiti, A., Kyritsakas, N. & Hosseini, M.W. (2007). Molecular tectonics on surfaces: Bottom-up fabrication of 1D coordination networks that form 1D and 2D arrays on graphite. *Angewandte Chemie—Int Ed* **46**(1–2), 245–249.

Wei, Z., Wang, D., Kim, S., Kim, S.Y., Hu, Y., Yakes, M.K., Laracuente, A.R., Dai, Z., Marder, S.R., Berger, C., King, W.P., De Heer, W.A., Sheehan, P.E. & Riedo, E. (2010). Nanoscale tunable reduction of graphene oxide for graphene electronics. *Science* **328**(5984), 1373–1376.

Xu, L., Miao, X., Ying, X. & Deng, W. (2012*a*). Two-dimensional self-assembled molecular structures formed by the competition of Van der Waals forces and dipole-dipole interactions. *J Phys Chem C* **116**(1), 1061–1069.

Xu, L., Miao, X., Zha, B. & Deng, W. (2012*b*). Self-assembly polymorphism: Solvent-responsive two-dimensional morphologies of 2,7-ditridecyloxy-9-fluorenone by scanning tunneling microscopy. *J Phys Chem C* **116**(30), 16014–16022.

Yan, L., Punckt, C., Aksay, I.A., Mertin, W. & Bacher, G. (2011). Local voltage drop in a single functionalized graphene sheet characterized by Kelvin probe force microscopy. *Nano Lett* **11**(9), 3543–3549.

Yang, Y., Miao, X., Liu, G., Xu, L., Wu, T. & Deng, W. (2012). Self-assembly of dendronized non-planar conjugated molecules on a HOPG surface. *Appl Surf Sci* **263**, 73–78.

Yilmaz, N., Ida, S. & Matsumoto, Y. (2009). Electrical conductivities of nanosheets studied by conductive atomic force microscopy. *Mater Chem Phys* **116**(1), 62–66.

Yoosaf, K., Ramesh, A.R., George, J., Suresh, C.H. & George Thomas, K. (2009). Functional control on the 2D self-organization of phenyleneethynylenes. *J Phys Chem C* **113**(27), 11836–11843.